

Control of a deformable mirror subject to structural disturbance

Matthew R. Allen, Jae Jun Kim, Brij Agrawal

Department of Mechanical and Astronautical Engineering, Naval Postgraduate School, Monterey,
CA, USA, 93943

ABSTRACT

Future space based deployable telescopes will be subject to non-atmospheric disturbances. Jitter and optical misalignment on a spacecraft can be caused by mechanical noise of the spacecraft, and settling after maneuvers. The introduction of optical misalignment and jitter can reduce the performance of an optical system resulting in pointing error and contributing to higher order aberrations. Adaptive optics can be used to control jitter and higher order aberrations in an optical system. In this paper, wavefront control methods for the Naval Postgraduate School adaptive optics testbed are developed. The focus is on removing structural noise from the flexible optical surface using discrete time proportional integral control with second order filters. Experiments using the adaptive optics testbed successfully demonstrate wavefront control methods, including a combined iterative feedback and gradient control technique. This control technique results in a three time improvement in RMS wavefront error over the individual controllers correcting from a biased mirror position. Second order discrete time notch filters are also used to remove induced low frequency actuator and sensor noise at 2Hz. Additionally a 2 Hz structural disturbance is simulated on a Micromachined Membrane Deformable Mirror and removed using discrete time notch filters combined with an iterative closed loop feedback controller, showing a 36 time improvement in RMS wavefront error over the iterative closed loop feedback alone.

Keywords: Adaptive Optics, Beam Control, Space Telescope, Wavefront Control

1. INTRODUCTION

The purpose of the research is to develop acquisition, tracking, and pointing technologies for future large aperture space telescopes and verify these technologies with the experimental test bed. The concept is to simulate an optical satellite payload with adaptive optics. The adaptive optics testbed uses a combination of deformable mirrors, tip/tilt fast steering mirrors, Shack-Hartmann wavefront sensors, and position sensing detectors to improve the quality of an imaged object. The light from the object of interest and a red reference laser travel together through the optical components of the testbed. Aberrations and disturbances can be input into the system through additional optical components or by a deformable mirror. A Shack-Hartmann wavefront sensor and position sensing detector sample the reference laser to provide feedback to a control algorithm to compensate for the aberrations.

This laboratory has historically studied attitude, pointing, and control methods for fine pointing of optical satellite payloads. The center has unique testbeds including 3-axis satellite simulators, an optical jitter control testbed using fast steering mirrors, and an adaptive optics testbed using deformable mirrors. Previous research has been conducted on vibration control of spacecraft optical payloads, optical laser pointing and jitter suppression, and jerk limited slew maneuvers of flexible spacecraft. Current work has focused on removing dynamic disturbances from a deformable mirror, by combining a gradient wavefront control technique developed by Zhu, Sun, Bartsch, Freeman, and Fainman with an iterative feedback controller as well as incorporating notch filtering techniques.

2. EXPERIMENTAL SETUP

The adaptive optics testbed is located in the Spacecraft Research and Design Center – Optical Relay Mirror Lab at the Naval Postgraduate School in Monterey California.

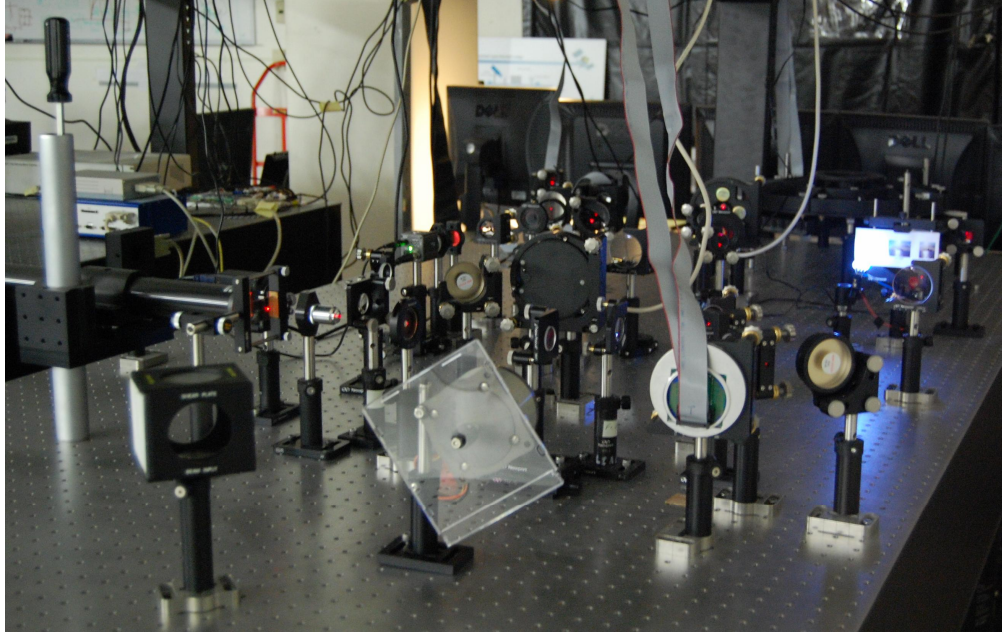


Fig. 1. Naval Postgraduate School Spacecraft Research and Design Center adaptive optics testbed

2.1. TESTBED DESCRIPTION

The components of the testbed are mounted on a Newport Optical Bench which can be floated to isolate the components from external vibrations. The concept is to simulate an optical satellite payload with deformable mirrors. The purpose of the testbed is to demonstrate advanced control algorithms that could be applied to an optical payload. The testbed is set up with three different control loops. The first control loop consists of a 15 mm OKO Technologies Micromachined Membrane Deformable Mirror (MMDM) and a hexagonal 127 lenslet Shack-Hartmann wavefront sensor. The first loop represents a primary deformable mirror on a space telescope and the control algorithms removes low frequency structural disturbances. The second control loop consists of two Baker Adaptive Optics Fast Steering Mirrors (FSMs) and a Position Sensing Detector (PSD). The second loop compensates for optical misalignment and controls tip/tilt aberrations attributed to jitter. The third control loop consists of a 30 mm OKO Technologies Piezoelectric Deformable Mirror (PDM) and a hexagonal 127 lenslet Shack-Hartmann wavefront sensor and is used to control higher order wavefront aberrations.

Lenses are used to manage the reference beam diameter and ensure that the reference laser beam is collimated. The lenses used in the testbed setup include a 20X microscope objective, and multiple doublets of different focal lengths. A microscope objective is the first lens and is used as a beam expander in the optical path of the reference beam to help ensure a planar wavefront. The microscope objective in combination with a doublet lens expands the beam to a one inch diameter beam. The doublet lenses are used to manage the diameter of the beam as it travels through the testbed. Beam splitters are used to divert a percentage of the reference beam in order for the sensors to provide measurements. Visible/infrared two inch diameter flat mirrors are used to redirect the beam to different components of the testbed. Figure 2 shows a schematic of the adaptive optics testbed.

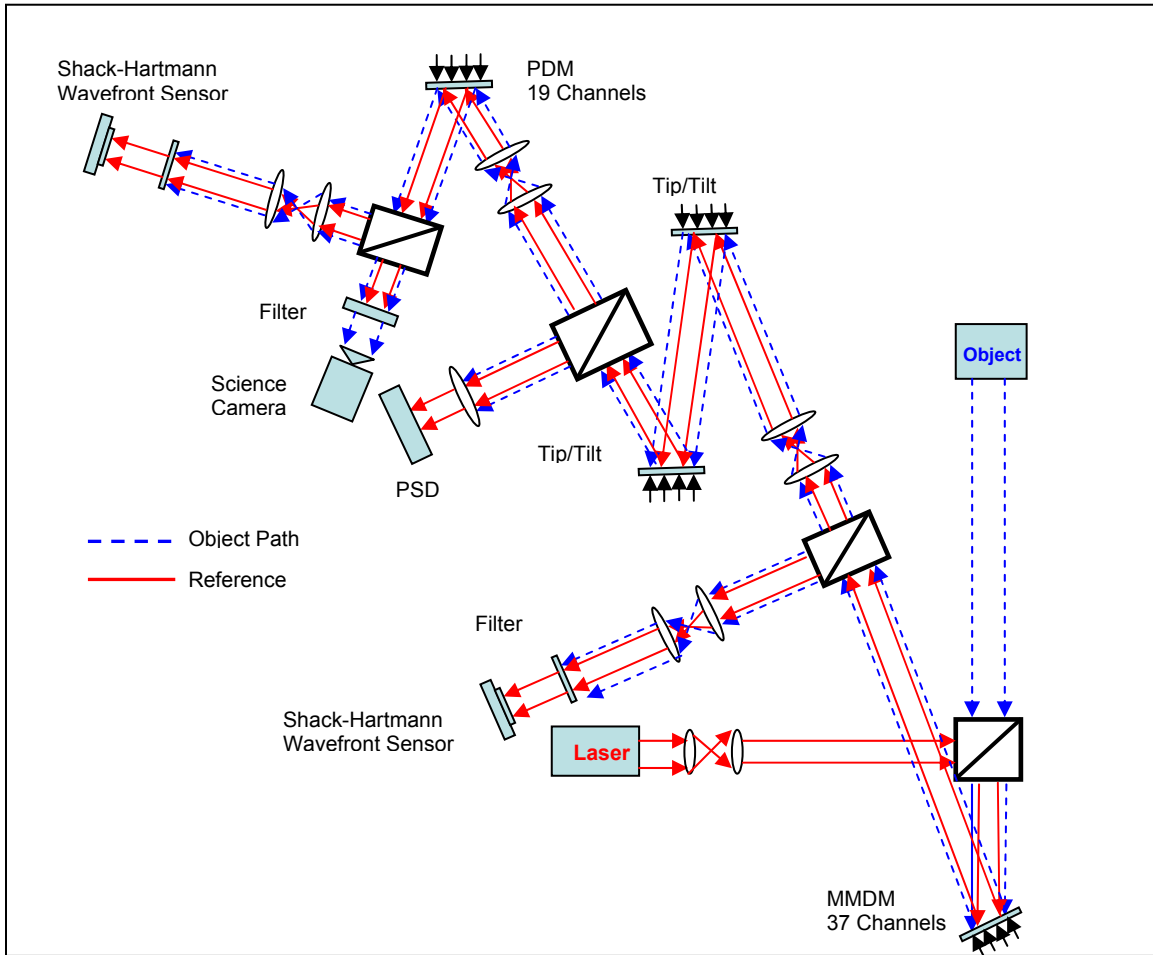


Fig. 2. Adaptive optics testbed schematic

2.2. Testbed operation

The experiments discussed in this paper only use the MMDM control loop to test adaptive optic control algorithms. The fast steering mirrors are adjusted such that their un-biased rest position allows the reference beam and object beam to pass through the optical system without any tip or tilt. A two inch flat mirror is then adjusted to ensure the reference beam is positioned on the center of the PSD. The third control loop with the PDM is not used.

2.3. Calibration and alignment

The performance of the adaptive optics system is dependent on the reference signal. In this case the reference signal is a planar wavefront produced by the reference laser. To ensure that the wavefront is planar the beam is expanded using the microscope objective and collimated with a lens. The collimation of the beam is checked using a sheer plate.

The collimated beam is required to calibrate the Shack-Hartmann wavefront sensors. The wavefront sensors operate based on the known positions of the lenslets on the Hartmann mask and their alignment with the camera sensor. To calibrate the wavefront sensor and remove any tip/tilt bias due to the optical components, a collimated beam was passed into the wavefront sensors and a reference image was captured. This reference image is used to measure the phase difference from a planar wave.

2.4. Data acquisition and MMDM drivers

The deformable mirrors are controlled using MATLAB. MATLAB interfaces to the deformable mirrors through a MATLAB executable (MEX) .dll developed by Baker Adaptive Optics. In this case C source code is converted to a C-MEX file to provide an external interface with the deformable mirrors. The MEX file is used in conjunction with the OKO Technologies MMDM and PDM drivers. The individual mirror actuators are addressed through MATLAB, and a control signal between 0 and 255 can be applied individually.

The wavefront sensors are also interfaced with MATLAB and use a C-MEX .dll to a memory mapped file. An executable file also developed by Baker Adaptive Optics, is used to perform the continuous image capturing directly to the computer RAM via the memory mapped file. This allows MATLAB to interface with the Basler A601f camera (used as the Shack-Hartmann wavefront sensor) through the Basler frame grabber driver using the 1394 firewire port.

3. CONTROL LAWS

3.1. System Model

The MMDM system can be modeled using a discrete time state space model, shown in Equations (1) and (2). In this model the state vector ϕ is the wavefront aberration, the matrix B is the influence matrix, the vector c is the vector of actuator control signals, the matrix Γ is a weighting matrix, the matrix S is the sensor operator, and y_k is the sensor output vector¹. The influence matrix B is determined experimentally and relates the control signal of an actuator to the change in the shape of the mirror. The weighting matrix is a constant matrix that weighs the importance of the previous states. In the adaptive optics system used in the experiments the weighting matrix is set to an identity matrix. Therefore no coupling or dynamics are assumed between the current state and the previous state. This assumption is appropriate as the frequency response of the deformable mirror used is very high at 500 Hz compared to the Shack-Hartmann wavefront sensor response of approximately 30 Hz.

$$\phi_{x,y,k+1} = \Gamma \phi_{x,y,k} + B_{x,y} [c] \quad (1)$$

$$y_k = S \phi_{x,y,k} \quad (2)$$

The discrete time state space model can also be used for a large mirror. However, a larger mirror will have a lower frequency response requiring the dynamics to be properly modeled. The system matrices will need to be determined experimentally or by a finite element analysis. Additional terms will also need to be added to include both the process noise and measurement noise. Despite the differences between the laboratory mirrors used in this experiment and a future large scale telescope the control law development is similar.

3.2. Wavefront reconstruction and estimation

The wavefront is approximated using a Zernike polynomial phase expansion, shown in Equation (3). Equation (3) can be written as a matrix where the individual phase points that describe the wavefront are contained in the vector $\phi(x, y)$, the Zernike coefficients are contained in vector \underline{a} , and matrix Z contains a matrix of M Zernike terms evaluated at the phase points x and y shown in Equation (4). Zernike polynomials are chosen because they are a set of orthogonal polynomials over the unit circle.

$$\phi(x, y) = \sum_{k=0}^M a_k z_k(x, y) \quad (3)$$

$$\underline{\phi}(x, y) = \underline{a}Z \quad (4)$$

A modal wavefront reconstruction is performed using the Shack-Hartmann wavefront sensor data. The Shack-Hartmann wavefront sensor measures the local slope of the wavefront. Taking the partial derivatives of Equation (3) represents a polynomial expansion of the wavefront slope, Equations (5) and (6), allowing the measured data to directly relate to the partial derivatives of the Zernike polynomials². Equations (5) and (6) can be written as a matrix where the vector \underline{S} is a column vector of both the measured x and y slopes, the matrix dZ contains a matrix of M derivative Zernike terms evaluated at the phase points x and y, and vector \underline{a} contains M Zernike coefficients. The coefficients can then be determined by performing a least squares fit and pre-multiplying both sides of Equation (7) by the pseudo inverse (represented by \dagger) of matrix dZ using a singular value decomposition. The piston component of the phase is lost through this reconstruction, but is not of concern². The wavefront reconstruction uses 21 Zernike coefficients throughout the experiment.

$$S^x = \sum_{k=1}^M a_k \frac{\partial z_k(x, y)}{\partial x} \quad (5)$$

$$S^y = \sum_{k=1}^M a_k \frac{\partial z_k(x, y)}{\partial y} \quad (6)$$

$$\underline{S} = [dZ] \underline{a} \quad (7)$$

$$\underline{a} = [dZ]^\dagger \underline{S} \quad (8)$$

3.3. Iterative feedback controller

Three control techniques were tested. The first control technique is an iterative closed loop feedback controller used throughout adaptive optics. The controller is similar to a closed loop proportional discrete time integral controller where a new control signal is updated based off the error multiplied by a proportional gain. The error is computed using the sensor data which is used to estimate the wavefront and compute the estimated residual wavefront aberration. The wavefront aberration is related to a control signal using an influence matrix which is determined experimentally resulting in Equation (9) where $\underline{\phi}$ is a vector of phase, B is the influence matrix, and \underline{c} is a vector of control signals to the mirror. The control signal representing the error is then multiplied by a gain, g . The resulting control law is shown as Equation (10). The block diagram is shown below and the plant can be represented by the influence matrix B , which models both the deformable mirror and the wavefront sensor. This control law is implemented using modal wavefront estimation techniques.

$$\underline{\phi} = B \underline{c} \quad (9)$$

$$\underline{c}_{n+1} = \underline{c}_n - g B^\dagger \underline{\phi}_n \quad (10)$$

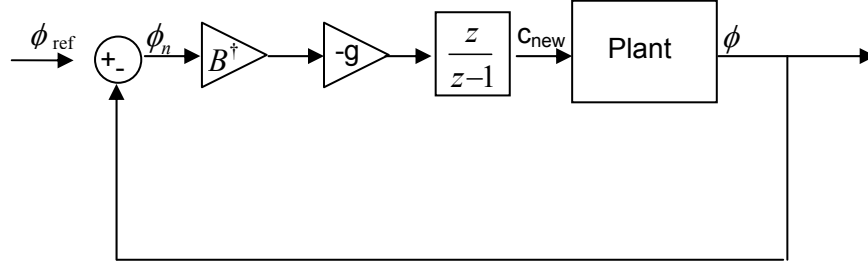


Fig. 3. Iterative Feedback Control

3.4. Combined iterative feedback and gradient feedback controller

The second controller combines the classic iterative closed loop feedback controller described previously with a gradient feedback controller. The resulting control law is shown in Equation (11). The wavefront is represented as a column vector of Zernike coefficients, \underline{a} , and therefore uses an influence matrix composed of Zernike coefficients, B_a , such that $a = B_a c$. The gradient is computed by taking the derivative of the wavefront variance over the circular aperture with respect to the control signal³. In Equation (11) μ is a scalar gain, \underline{w}^2 is a vector of coefficients computed by integrating each Zernike term over the unit circle, B_a^T is the transpose of B_a , and $*$ denotes an element wise vector multiply.

$$\underline{c}_{n+1} = \underline{c}_n - g B_a^\dagger \underline{a} - 2\mu B_a^T (\underline{a} * \underline{w}^2) \quad (11)$$

3.5. Discrete time notch filter

The third controller combines a classic iterative closed loop feedback controller with a notch filter. The notch filter is applied to control resonant peaks and known frequencies that excite the structure. A structure with low damping may lead to increased resonant peaks in the frequency response of the structure causing potential wavefront error as the mirror surface dynamically changes. External narrowband disturbances are also of concern as they can impart a disturbance on the structure. Second order structural filters can be applied to compensate for known resonant frequencies.

In order to implement a notch filter on the experimental testbed a discrete time notch filter is required. A second order notch filter in the Z-domain is presented in Equation (12) where ω_n and BW are the normalized central angular frequency and bandwidth of the notch filter⁴. This notch filter can be applied to an individual actuator control signal, requiring a notch filter on each control channel of the deformable mirror to remove known narrowband disturbances. The notch filter is implemented on the testbed using Equation (15) where $y(n)$ represents the current output and $u(n)$ is the current control input.

$$H_z(z) = \frac{1}{2} \left[1 + \frac{k_2 + k_1(1 + k_2)z^{-1} + z^{-2}}{1 + k_1(1 + k_2)z^{-1} + k_2z^{-2}} \right] \quad (12)$$

where,

$$k_1 = -\cos(\omega_n) \quad (13)$$

$$k_2 = \frac{1 - \tan\left(\frac{BW}{2}\right)}{1 + \tan\left(\frac{BW}{2}\right)} \quad (14)$$

$$y(n) = -k_1(1+k_2)y(n-1) - k_2y(n-2) + \frac{1+k_2}{2}u(n) + k_1(1+k_2)u(n-1) + \frac{(k_2+1)}{2}u(n-2) \quad (15)$$

4. RESULTS

The performance of the control algorithms is measured by the root mean square (RMS) wavefront error. The RMS wavefront error is the square root of the variance of the wavefront and is calculated over the normalized aperture using Equation (16). In all the experiments the error of the wavefront is only calculated over 85% of the Hartmann mask aperture using a diameter of 3 mm. This eliminates the outer fringes of the wavefront as the MMDM deformation range is limited at the outer edges since the membrane is fixed at the boundary.

$$\sigma_\phi = \sqrt{\frac{1}{\pi} \int_{-1}^1 \int_{-\sqrt{1-x^2}}^{\sqrt{1-x^2}} [a_k z_k(x, y)]^2 dx dy} = \sqrt{a_k \frac{1}{\pi} \int_{-1}^1 \int_{-\sqrt{1-x^2}}^{\sqrt{1-x^2}} [z_k(x, y)]^2 dx dy} = \sqrt{a_k^2 w_k^2} \quad (16)$$

The iterative feedback, gradient feedback and combined controllers were applied to the MMDM to correct the mirror surface from a biased position with a RMS wavefront error of 10.96 and a 5 Hz sinusoidal disturbance on the 37 actuators. The control algorithms were configured to drive the mirror from the biased position to a position resulting in a planar wavefront.

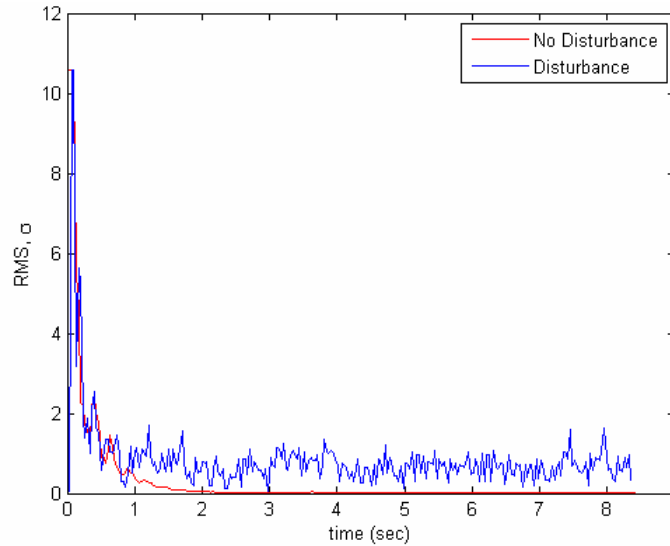


Fig. 4. Wavefront error history using an iterative feedback controller with modal phase estimation with and without a 5Hz sinusoidal disturbance

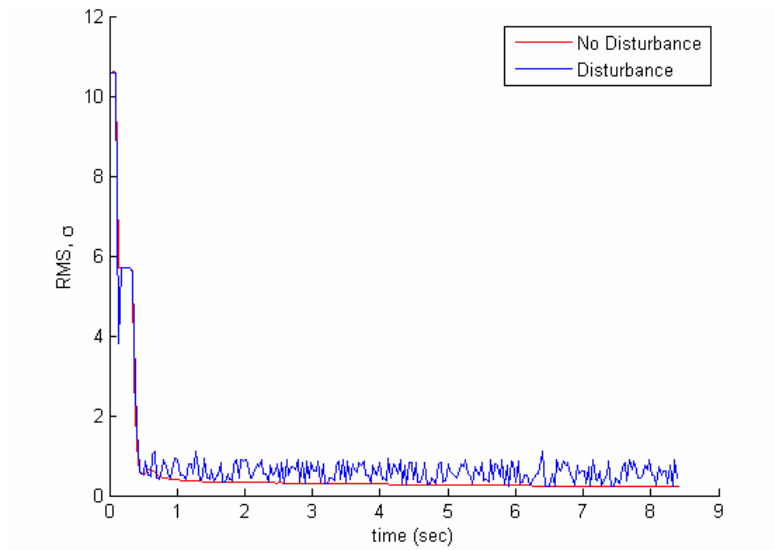


Fig. 5. Wavefront error history using an iterative gradient feedback controller with modal phase estimation with and without a 5Hz sinusoidal disturbance

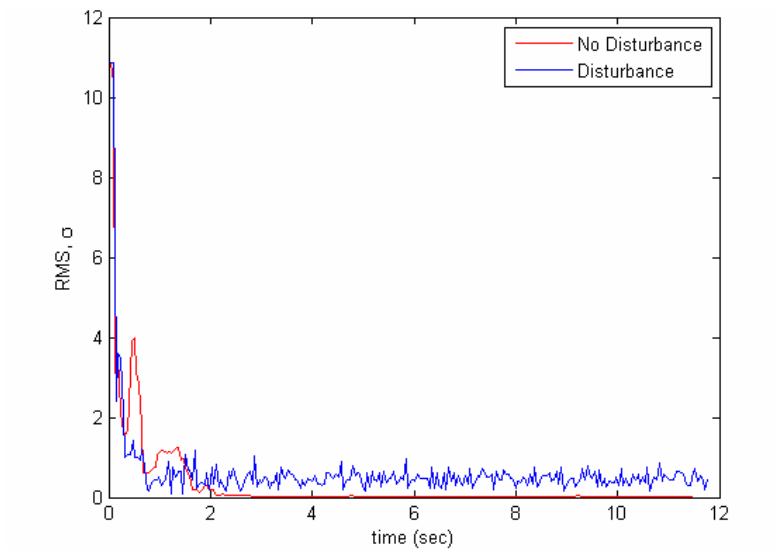


Fig. 6. Wavefront error history using a combined iterative feedback and iterative gradient feedback controller with modal phase estimation with and without a 5Hz sinusoidal disturbance

Table 1. Steady state RMS wavefront error for MMDM from a biased position without disturbance and with a disturbance.

Controller	σ (Biased)	σ (Biased and 5Hz Disturbance)
Iterative Feedback Controller	0.028	0.8897
Iterative Gradient Feedback Controller	0.10174	1.95
Combined Controller	0.00619	0.8547

A 2 Hz sinusoidal disturbance and a discrete time notch filter were also applied to all the actuators starting from the same biased position. The filter bandwidth is set to 0.1π .

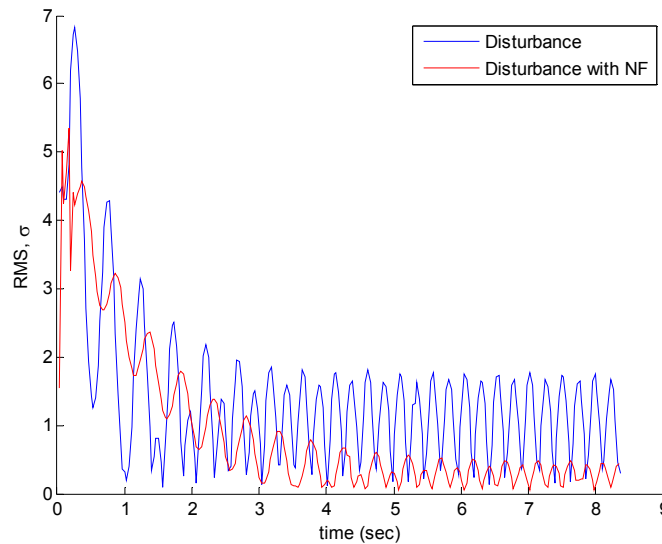


Fig. 7. Wavefront error history using an iterative feedback controller subjected to a 2Hz sinusoidal disturbance on all 37 MMDM actuators with and without a notch filter

In the last experiment a simulated structural disturbance is introduced into the mirror with a sinusoidal disturbance in the third Zernike term which represents focus. This creates an oscillating focus aberration on the surface of the mirror and in the wavefront. The disturbance simulates a first mode vibration disturbance across the face sheet at a specific frequency. Unlike the previous notch filter experiment where each actuator had the same disturbance signal, the actuator voltages are adjusted to achieve the desired wavefront and mirror aberration. The second order notch filtering techniques previously developed are applied to the iterative feedback control law to reduce the disturbance.

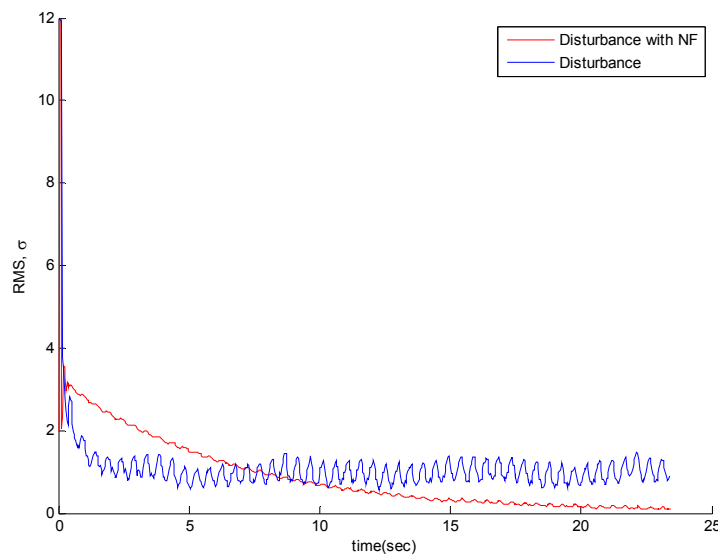


Fig. 8. Wavefront error history using an iterative feedback controller subjected to a 2Hz sinusoidal disturbance on wavefront focus with and without a notch filter

The resulting error history for the disturbance shows that the notch filter was able to successfully remove the simulated disturbance using a bandwidth of 0.8π . The resulting steady state RMS wavefront error is comparable to the corrected wavefront results achieved without a disturbance but at the cost of a greater settling time.

Table 2. Steady state RMS wavefront error for MMDM from a biased position subjected to a 2Hz disturbance using notch filtering techniques.

Experiment	Bandwidth of		
	NF	σ without Filtering	σ with Filtering
2 Hz Disturbance on 37 Actuators	0.1π	1.778	0.483
2 Hz Simulated Structural Vibration	0.8π	1.47	0.0405

5. CONCLUSIONS

The experimental results showed that a combination of an iterative feedback and gradient feedback control law using variance minimization provided the smallest RMS wavefront error when correcting from a biased position and when correcting the mirror subjected to a sinusoidal noise disturbance. However the combined controller is very sensitive to the gains, requiring both the iterative gain and the gradient feedback gain to be properly tuned. All the control algorithms showed a residual disturbance in the wavefront error when subjected to a sinusoidal disturbance, when filtering techniques were not applied.

The experimental results demonstrated that a second order discrete time notch filter can be used in the adaptive optics control algorithm to improve the steady state RMS wavefront error when a known constant frequency disturbance is present. Applying a properly tuned notch filter in series with a controller decreased or removed the dynamic disturbance. The notch filter success in the experimental work was dependent on knowledge of the disturbance frequency, the notch filter bandwidth, and the knowledge of the computer sampling time. The experimental work successfully demonstrated that low frequency filtering of actuator noise as well as a simulated structural disturbance achieved a wavefront error comparable to results achieved without a disturbance.

6. REFERENCES

- [1] Frazier, B. W. and Tyson, R. K., "Robust control of an adaptive optics system," Proceedings of the Thirty-Forth Southeastern Symposium on System Theory, 293-296 (2002).
- [2] Southwell, W.H., "Wave-front estimation from wave-front slope measurements," Journal of the Optical Society of America. 70(8), 998-1006 (1980, August).
- [3] Zhu, L., Sun, P. C., Bartsch, D. U., Freeman, W. R., and Fainman, Y., "Adaptive control of a micromachined continuous-membrane deformable mirror for aberration compensation," Applied Optics. 38, 168-176 (1999, January).
- [4] Hsue, C. W., Chen, Y.J., and Tsai, Y. H., "Design of bandstop filters using discrete time notch filter, two section stub, and frequency-scaling method," Microwave and Optical Technology Letters. 49, 1098-1101 (2007, May).